

Vertical Taper InGaAsP/InP Fabry-Perot Laser Diode for Injection-Locking Applications in WDM-PON Systems

Joni Welman Simatupang¹

Assistant professor

¹*Electrical Engineering Study Program,
Faculty of Engineering, President University, Indonesia.*

Abstract

The cost effective and wavelength stability of laser light sources are critical issues for practical implementation of wavelength division multiplexing-passive optical network (WDM-PON) technology. This paper explains the optimized laser structure design and fabrication process to realize the Fabry Perot-Laser Diode (FP-LD) with vertical tapered-waveguide by diffusion-limited etching as a simple and low cost fabrication method. Then, it will be applied to the injection-locking technique to produce the single-mode operation wavelength that finally can be used as a low cost optical network unit (ONU) light source in a WDM-PON system. After injection-locking measurements, the output wavelength of the 500 μm total cavity length with 200 μm taper region which produces 8.566 mW output power and 16% slope efficiency FP-LD is locked to the externally injected light from tunable laser source. The measured of the best side mode suppression ratio (SMSR) is higher than 30 dB. This value is sufficient to be used for WDM-PON applications in “the third window” of optical fiber communication systems.

Keywords: vertical taper, FP-LD, injection-locking measurement, diffusion-limited, WDM-PON systems.

I. INTRODUCTION

1) Semiconductor Laser Diodes

The unique properties of semiconductor materials have enabled the development of a wide variety of ingenious (cleverly made or planned involving new ideas and methods) devices that have literally changed our world today. These devices have been studied for more than 135 years since 1874 when Braun invented the metal-semiconductor contact device. Now, there are about 60 major devices or more with over 100 device variations related to them. One of the remarkable progresses

(discoveries) was the invention of semiconductor laser diode by Hall et al. in 1962. Semiconductor laser diode is the class of lasers in which the coherent optical emission is originated from the stimulated transition from a higher energy band (conduction band) to a lower energy band (valence band). A year later (1963), three Russian's scientists: H. Kroemer, Zh.I. Alferov, and RF.Kazarinov proposed the heterostructure laser composition. These proposals laid the foundation for modern laser diodes, which can be operated continuously at room temperature. Laser diodes are the key components for a wide range of applications, including CD players, digital video disks (DVDs), laser printing, atmospheric pollution monitoring, and optical-fiber communication systems (May and Sze, 2004 and Cloutier, ELEG340).

The main features that distinguish the semiconductor laser diodes from other type of lasers are (Yariv and Yeh, 2007):

1. Small physical size ($300\ \mu\text{m} \times 10\ \mu\text{m} \times 50\ \mu\text{m}$) that enables it to be incorporated easily into other instruments.
2. Its direct pumping by low-power electric current (typically is 15mA at 2V), which makes it possible to drive it with conventional transistor circuitry.
3. Its efficiency in converting electric power to light. Actual operating efficiencies exceed 50%.
4. The ability to modulate its output by direct modulation of the pumping current at rates exceeding 20 GHz. This is the major importance in high-data-rate optical communications systems.
5. The possibility of integrating it monolithically with electronic field effect transistors, microwave oscillators, bipolar transistors, and optical components in III-V semiconductors to form integrated optoelectronic circuits.
6. The semiconductor-based manufacturing technology, which lends itself to mass production.
7. The compatibility of its output beam dimensions with those of typical silica-based optical fibers and the possibility of tailoring its output wavelength to the low-loss ($\lambda=1.5\ \mu\text{m}$) and low-dispersion ($1.3\ \mu\text{m}$) region of such fibers. For long distance applications, laser diodes are preferred compared to LED (Light Emitting Diodes) due to their higher output power, spectral purity, higher efficiency, and easier coupling into optical fibers.
8. The possibility of tailing its output wavelength to the blue spectral regime for display and the readout of high-density optical storage.

What processes are required to construct these wondrous devices from basic semiconductor materials? As for IC (integrated circuit) fabrication, there are five major steps to produce laser diode devices. These steps are oxidation, photolithography, etching, ion implantation, and metallization. Lithography is a key technology for semiconductor industries. The continued growth of the industry has been the direct result of improved lithographic technology. *Lithography* is also a significant economic factor that currently representing over 35% of IC manufacturing

costs. *Epitaxy*, derived from the Greek words *epi*, meaning “on” and *taxis*, meaning “arrangement,” describes a technique of crystal growth to form a thin layer of semiconductor materials on the surface of a crystal that has a lattice structure identical to that of a crystal. This method is important for the improvement of device performance and the creation of novel device structures. As the device dimensions were reduced, the dry etching technique was developed to replace the wet chemical etching for high-fidelity pattern transfer. Device miniaturization results in reduced unit cost per circuit function. For example, the cost per bit of memory chips has halved every 2 years (Moore’s Law) for successive generations of DRAM (digital random access memory) circuits. As device dimensions decrease, the intrinsic switching time decreases. Device speed has improved by four orders of magnitude and beyond for more than 50 years. As device becomes smaller, they consume less power. Therefore, device miniaturization also reduces the energy used for each switching operation. And computational power also increases by a factor of 2 every 18 months (May and Sze, 2004).

The successful fabrication of a laser diode relies very heavily upon the properties of the materials involved. There is a very limited set of semiconductors that possess all of the necessary properties to make a good laser. For the desired double heterostructures, at least two compatible materials must be found, one for cladding layers and another for the active region. In more complex geometries, such as SCH (separate confinement heterostructure), three or four different bandgaps may be required within the same structure. The most fundamental requirement for these different materials is that they have the same crystal structure and nearly the same lattice constant, so that single-crystal, defect-free films of one can be *epitaxially* grown on the other. Defects as well as Auger processes and surface recombination generally become the nonradiative recombination centers which can steal many of the injected carriers that otherwise would provide gain and luminescence (Coldren and Corzine, 1995).

2) Fabry-Perot Laser Diode (FP-LD)

The most common communication laser is called the “Fabry-Perot” laser. The Fabry-Perot laser diode (FP-LD) is conceptually just an LED (light emitting diode) with a pair of end mirrors. On the surface of it, an FP-LD should be easier to construct than LED. In LED someone has to give a lot of attention to collecting and guiding the light within the device towards the exit aperture. In an ideal laser, actually you don't have the problem of guiding the light at all. Lasing takes place only between the mirrors and the light produced is exactly positioned. The mirrors are needed to create the right conditions for lasing to occur. In practice of course it is somewhat more complex than this - but not a lot. Fabry-Perot laser gets its name (and its operational principle) from the fact that its cavity acts as a Fabry-Perot resonator or Fabry-Perot filter (etalon). Having said that, we can also say that the Fabry-Perot laser is a Fabry-Perot interferometer which includes an active medium between the two mirrors; of course, the active medium should be able to amplify the light (Dutton, 1998).

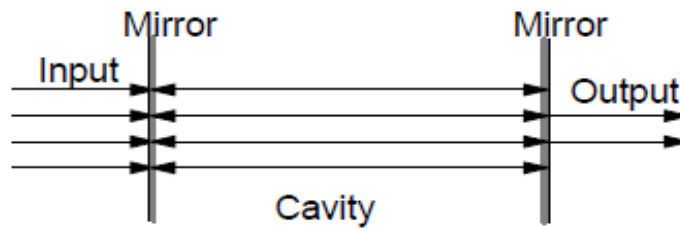


Figure 1. Fabry-Perot Filter (Dutton, 1998).

Light enters the cavity through a partially silvered mirror on the left and leaves it through a partially silvered mirror on the right. Only wavelengths that resonate within the cavity are able to pass through. Other wavelengths are strongly attenuated.

It is expected that the laser to be “Fabry-Perot” when it has a relatively short cavity (in relation to the wavelength of the light produced). Wavelengths produced are related to the distance between the mirrors by the following formula:

$$Cl = \frac{\lambda m}{2n}$$

where Cl = length of the cavity,

λ = wavelength,

m = an arbitrary integer: 1, 2, 3,..

n = refractive index of the active medium.

To understand the operation of the Fabry-Perot laser it is first necessary to understand the Fabry-Perot filter. The principle of the Fabry-Perot filter is illustrated in Figure 1. When you put two mirrors opposite one another they form a resonant cavity. Light will bounce between the two mirrors. When the distance between the mirrors is an integral multiple of half wavelengths, the light will reinforce itself. Wavelengths that are not resonant undergo destructive interference with themselves and will be reflected away.

3) Taper Waveguide and Etching Technique

In a conventional laser diode, optical confinement in the semiconductor structure is asymmetric and the propagating mode profile is elliptical in shape. This highly divergent and elliptical output beam profile faced difficulty when coupled to the single mode optical fiber. This difficulty caused by the large mode mismatch between the semiconductor laser source and the optical fiber.

Several approaches have been employed to improve the chip-fiber coupling efficiency such as using micro-lenses or tapered fibers and the insertion of silica-based

waveguide module containing a mode-field converting waveguide. The former approaches still suffer from the field mismatch problem because only the size of the optical mode is converted. And the latter approach still hinders the easy and low cost packaging because the small alignment tolerances at the III-V semiconductor interface happened, although good mode-matching and high-coupling efficiencies can be obtained. According to all weaknesses mentioned before, many researchers for almost three decades have been focused their research on the monolithic integration of mode size converters (tapers) with III-V semiconductor components to improve the output coupling fiber in order to achieve a larger and more symmetric near field pattern (NFP) at the device facet. Spot size converters (SSCs) or tapers were made to increase the spot size on the chip in order to minimize the in- and out-coupling loss. This approach allows both the low coupling loss and large alignment tolerances and therefore reduced the packaging cost.

Many researchers have been tried to improve the light coupling efficiency between optical fibers and semiconductor waveguides by designing many different types of tapers: lateral, vertical, combined, and special ones. These efforts made taper waveguides have Gaussian mode-profile at the end of the output facet that are fully matched (minimum loss field mismatch) to the fiber optical mode. In this time, thorough explanation of all taper designs will not provided because readers can fully read it through Ref (Moerman, *et al.*, 1997), but we limit ourselves in this section by only describing the lateral and vertical tapers layout. It is also out of our concern and capacity to discuss the taper design rules or to define the optimal taper dimensions, although we have learned a few about that knowledge in (Hadley, 1993).

4) Lateral Taper

In lateral taper designs, the width of the guiding layers is changed (smaller or larger than before) without affecting the vertical waveguide structure. There are many kinds of structures from the simple designs to the complicated ones, such as lateral down- or up-tapered buried waveguide, single and multi-section taper transition from a ridge waveguide to a fiber-matched waveguide, dual lateral overlapping buried or ridge waveguide taper, and nested waveguide taper transition from a ridge waveguide to a fiber-matched waveguide.

Lateral mode conversion tapered waveguides that adiabatically increase or decrease in the width have been proposed in the past time to improve the mode shape of the semiconductor waveguide when coupled into the fiber. Early investigations theoretical work have shown that two-dimensional lateral tapers provide 90% coupling efficiency (power or energy conversion) and more complicated taper shapes-such as parabolic, exponential, Gaussian, and hyperbolic-increase this percentage by modest amounts (Ladele, *et al.*, 2001 and Choudhury, *et al.*, 2005). The reason why many researchers have developed such lateral tapers is the relatively easy in fabrication that can use standard binary lithography techniques. However, lateral tapers help in matching the modes only in the lateral direction, but the mismatch in vertical direction still remains.

5) Vertical Taper

Vertical structure has a lot of applications to the optoelectronic integrated circuits (OEIC). Different with lateral tapers, in a vertically tapered waveguides, the thickness of guiding layers is changed along the device (can be linear, exponential, or parabolic shapes). Also, the special growth and etching techniques are required to change the thickness along the taper.

To our knowledge, there are at least five designs of one-dimensional vertical tapers, such as: vertical down-tapered buried waveguide, vertical down-tapered ridge waveguide, vertical overlapping ridge waveguide taper, vertical overlapping waveguide taper transition from a buried waveguide to a fiber-matched waveguide, and vertical overlapping waveguide taper transition from a ridge waveguide to a fiber-matched waveguide. For all kinds of vertical taper designs, we knew that the only critical issue for the taper fabrication is the thickness control of the tapered waveguide.

6) Etching Technique

Many etching techniques like dip-etch process, dynamic etch mask technique, diffusion limited etching technique, stepped etching, and sputtering etching were proposed to fabricate the vertically tapered structures. All of these wet etching techniques have disadvantages of either low reproducibility or high time consumption and the difficulty to define the sophisticated taper profiles such as parabolic or exponential shapes. Although more difficult, the non-linear vertical taper profiles are often recommended to reduce the taper length.

A taper region in a semiconductor waveguide device acts to adiabatically control the expansion of propagating wave and therefore, the resultant mode-size of the guided optical wave. These tapers maybe fabricated by various techniques and often designed to have a Gaussian mode-profile at the waveguide output facet. In this paper, our concern is mostly given to the vertical taper design and fabrication method, especially for the vertical down-tapered buried waveguide by diffusion-limited etching as a simple and low-cost fabrication technology.

7) Wavelength Division Multiplexing-Passive Optical Network (WDM-PON)

Passive optical network (PON) is a point-to-multipoint optical network, where an optical line terminal (OLT) at the central office (CO) is connected to many optical network units (ONUs) at the end-subscribers through optical splitters or AWG (array wavelength grating) at the remote node (RN). PON have evolved to provide much higher bandwidth in the access network. PON also offers additional advantages like high reliability and easy maintenance. These characteristics are important for access network deployment such as fiber-to-the curb, fiber-to-the building, and fiber-to-the-home.

Well-developed wavelength division multiplexing (WDM) technology can be added to a PON to vastly increase the overall capacity. In a WDM-PON technology, different subscribers are assigned to a distinct or dedicated wavelength channels (Figure 2). These channels are routed by a passive wavelength routing device located at a remote node (RN) that is close to the customer premises.

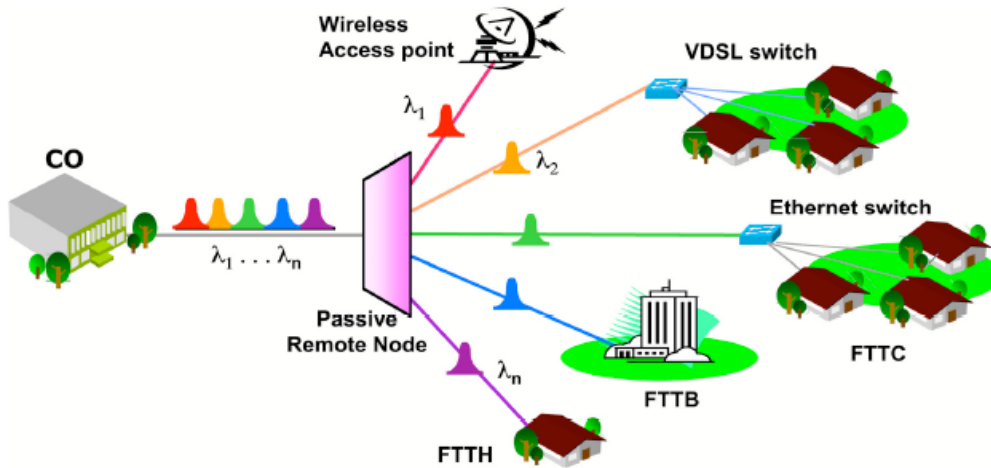


Figure 2. WDM-PON supports multiple subscribers (Novera Optics, Inc).

This virtual point-to-multipoint PON architecture enables (Novera Optics, Inc): (a) large guaranteed bandwidths, (b) bit rate independency, (c) protocol transparency, (d) graceful upgradeability, (e) high QoS (Quality of Service), and (f) excellent security and privacy. In addition to increasing network capacity, WDM-PON also eliminates the power splitting loss and enhances the privacy of end users. However, the cost-effective and wavelength stability of light sources are the critical issues for practical implementation of WDM-PON technology, especially for customer premises equipment.

Several light sources have been considered so far, like spectrum-sliced light-emitting diodes (LEDs), amplified spontaneous emission (ASE) source from an erbium doped fiber amplifier (EDFA), wavelength seeded reflective semiconductor optical amplifiers (RSOAs), self seeding SOAs, spectrum-sliced free running Fabry-Perot Laser Diodes (FP-LDs), and a light source for receiving downstream signals for remodulation. The methods using LEDs and SOAs suffer from low power budget and high packaging cost, respectively. Also, the methods using the spectrum slicing of a free-running FP-LD suffers from strong intensity noise, while the remodulation method needs further development to suppress the crosstalk from residual downlink data and to reduce the dependence of polarization state of the downlink signal (Xu, *et al.*, 2007).

Because of its low-cost and facilitated production, FP-LD is very desirable, but the multimode operation limits its applications. Optical injection is an attractive and

effective method to modify its characteristics, such as reducing the nonlinear distortion, the mode partition noise, and the chirp, and also improving the modulation bandwidth, the side mode suppression ratio (SMSR), the 3 dB bandwidth and the wavelength output stability.

8) Injection-Locking FP-LD

Optical injection-locking is a long studied technique related to all-optical communication and signal regeneration fields. Injection locking where the optical oscillation light in the slave laser is locked to a stable master signal, has been applied to many areas such as turning the multimode FP-LD to be the single-mode operation wavelength, to stabilization of lasers, wavelength conversion, modulation response of incoherently injection-locked, reducing the mode partition noise, reducing the nonlinear distortion, WDM-PON spare function and improving the modulation bandwidth. In this paper, FP-LD with vertical tapered-waveguide by diffusion-limited etching as a simple and low cost fabrication method has been applied to the injection-locking technique using the tunable laser light to produce the single-mode operation wavelength that can be used as a low cost light source for a moderate speed in WDM-PON system.

II. FABRICATION PROCESS

1) Vertical Taper Design Structure

InGaAsP/InP is one of the basic material systems of modern optoelectronics. Well developed and mature MOCVD (metal organic chemical vapor deposition) technology allows for high yield fabrication of lasers in the wavelength range 0.97 and up to 2 μm for telecommunication and other needs. The main peculiarity of devices based on InGaAsP is a relatively small conduction band offset; about 60% of the net band offset is valence band offset. The high mobility electrons, together with a small confinement barrier will make the carrier leakage through thermionic emission as a serious concern.

So, the ridge-waveguide structure was optimized to reduce the leakage current and leading to the high injection efficiency. The price paid for this advantage is an increased optical loss due to the free carrier absorption. Alternatively, waveguide broadening minimizes optical loss due to the decreased overlap of the optical mode with the highly doped cladding regions. The trade-off between increased loss and the reduction of carrier leakage from the active region governs the laser design [Belenky, *et al.*, 2002].

We designed a device structure of the linear vertical down-tapered ridge-waveguide MQW FP-LD (Figure 3). The structure is designed for use in the third window optical communication at 1550 nm wavelength region. By using the diffusion-limited etching, the thickness of 0.7 μm sacrificial layers (cladding InP and InGaAsP SCH layers) are gradually reduced in the vertical direction.

This MQW layers consists of four 60Å unstrained InGaAsP wells ($\lambda_{EL}=1.55\mu\text{m}$) and five 100Å InGaAsP barriers ($E_g=0.954\text{ eV}$). A compressive strain of 1% and a tensile strain of 0.2% are incorporated in the QWs and the barriers, respectively are used to reduce the internal losses. The MQWs are sandwiched by an undoped InGaAsP 500Å thick lattice-matched lower separate confinement heterostructure (SCH) layer and undoped 0.25 μm thick lattice-matched upper graded index (GRIN-) SCH layers where its energy bandgap is linearly changed from 1.0Q to 1.3Q. The (Q1.3) notation implies the quaternary InGaAsP with 1.3 μm bandgap wavelength. These GRIN-SCH layers were employed to obtain the efficient carrier injection and high quantum efficiency. According to the current injection efficiency analysis (Kunii, *et al.*, 1995 and Hirayama, *et al.*, 1992), the efficiency of linear GRIN-SCH is the highest between step-, parabolic GRIN- and linear GRIN- structures with the same well depth.

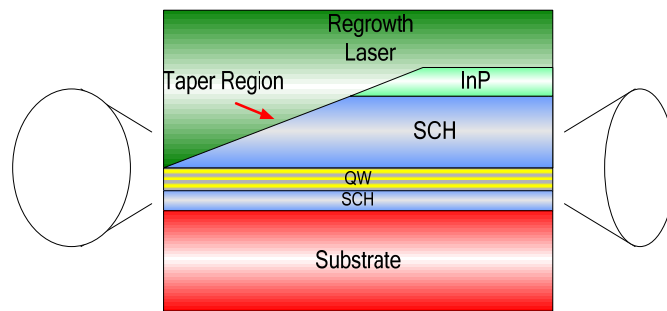


Figure 3. Schematic drawing of the realized vertical taper laser.

2) Diffusion-Limited Etching Method

Similar to the MOVPE (Metal-Organic Vapor Phase Epitaxy) process in which the growth rate will be enhanced when the substrate is covered by a dielectric mask (because no deposition takes place on the dielectric mask): “the larger the mask width, the smaller the mask window; the higher the reactor pressure, the larger the growth rate enhancement,” the diffusion-limited etching technique also working on the same principle. (Moerman, *et al.*, 1994)

In a diffusion-limited etching method (Simatupang *et al.*, 2009), the etching rate is controlled by mass transport of reactants to the surface or product from the surface. This method is relatively not sensitive to the temperature but highly sensitive to changes in nature and degree of agitation. Diffusion-limited etching has been used for long time to fabricate the optoelectronic integrated circuits in the III-V compound semiconductor material system, both for large area as well as for controlled local area depth etching.

3) Mask Pattern Design (Test and Real Samples)

Our etching test mask design (Figure 4) is quite similar to the mask design that was made by Brenner and Melchior (Brenner and Melchior, 1994). The masking stripes

consists of 1000 μm length SiO_2 running along the entire length of chip, have a gap width (W_g) of 10, 20, 40, 80, 100 μm and a mask width (W_m) of 10-100 μm at a repetition period of 250 μm . Then the test samples were etched by bromine-acid solution ($\text{HNO}_3:\text{HBr}:\text{H}_2\text{O} = 5:5:250$) under different conditions. By using stylus profiler (α -step measurement system), the etching depth was measured and it was found that the higher etching rate is found in the smaller gap width ($W_g=10 \mu\text{m}$) with the bigger mask width ($W_m=100 \mu\text{m}$), according to its principle. We choose the 20 μm gap width (W_g) for our real samples with the taper lengths are vary from 100, 200, 300, to 500 μm as it is shown in mask pattern design (Figure 5). So, the mask contains the fixed spacing (W_g) and laterally increasing width and length along the taper mask (W_m).

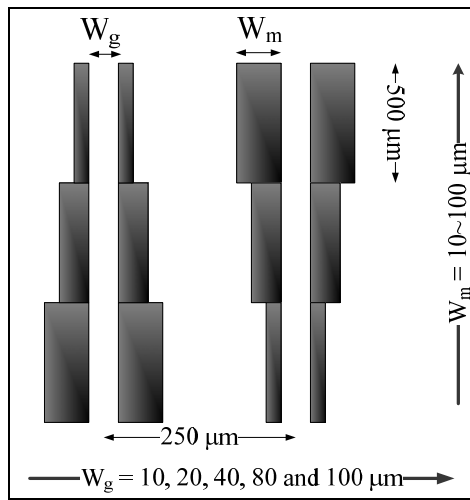


Figure 4. Mask layout for local area test etching rate of InP/InGaAsP by bromine-nitrid acid solutions.

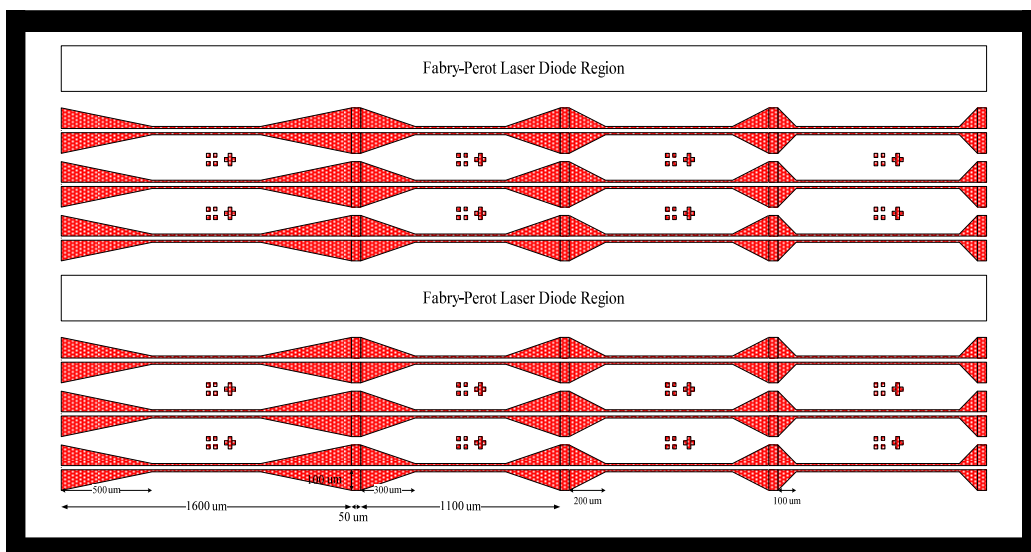


Figure 5. Fabry-Perot Laser Diode (FP-LD) Design.

4) Ridge-Waveguide Fabrication

In this fabrication step, *multilayers* were grown on the InP substrate with the core active layer by MOCVD. Then a 20 μm gap width silicon dioxide mask pattern was transferred to the sample. By diffusion-limited bromine-acid solutions, the epitaxial layers were etched with the trenches of removed material becoming gradually deeper as *the length of taper region become longer*, leading to the desired vertical tapers. Then, we removed the SiO₂ mask pattern using BOE (Buffered Oxide Etch) solution for 3 minutes for each of sample and then put to DI (*deionized*) water for 5 min. The bromine etching left a smooth and damage-free surface, suitable for the *epitaxial re-growth*.

Following, the photolithography was performed process to define the pattern. Firstly, spin coating PR was employed using HMDS & AZ5214E solutions with certain conditions: pressure (35-40W), period (± 2000 rpm), and time (45 sec.), then followed by soft-bake at 110°C for 50 sec. Secondly, by mean of contact aligner (Karl-Suss MJB 3), we exposure the sample for 2 minutes to remove edges part (and development for 1.5 min.) and 12 sec. to transfer the 2 μm ridge pattern (development for 40 sec.), then put to DI water for 30 sec.

The fabrication process until ridge-waveguide definition was well done (Figure 6) and going to step forward for the next process.

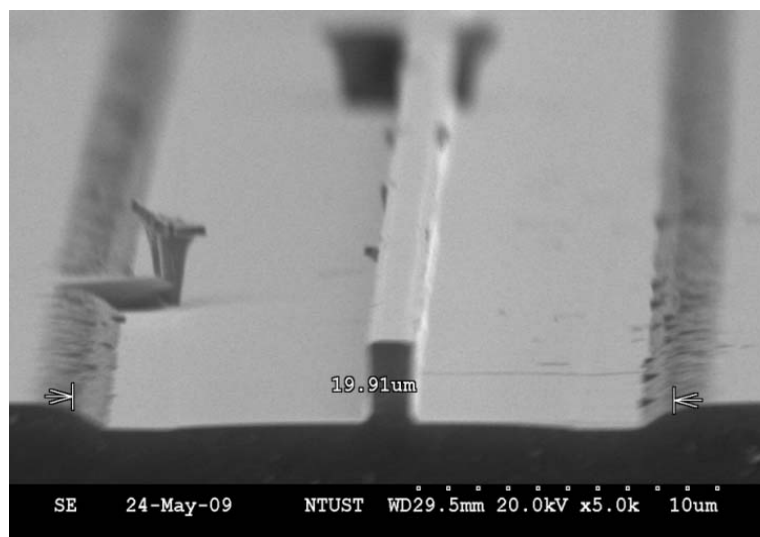


Figure 6. Smooth taper ridge-waveguide, the width $\cong 20 \mu\text{m}$ and the depth $\cong 2.5 \mu\text{m}$.

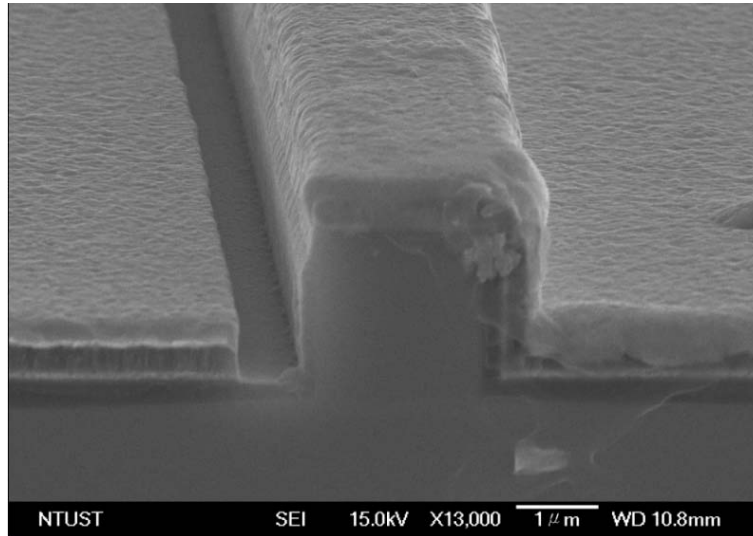


Figure 7. Tapered laser shows the uniformity of P-metal coating on the ridge top surface and good SiO₂ isolation layer below it.

5) Epitaxial Regrowth, Self-Alignment, Metallization Contact, RTA Process

After epitaxial regrowth process finished in three weeks, we continue to do the self alignment. This process is begun by coating the SiO₂ using PECVD (phase epitaxy chemical vapor deposition) technique and SiO₂ becomes the isolation layer which covering on top of the ridge-waveguide surface. Metallization process is known as the image reversal technique: transferring the p-metal pattern into the sample surface by exposure, soft-bake reversal, and RIE (reactive ion etching) plasma process. Then, by using the electron beam evaporation gun (E-gun), the metal Ti/Pt/Au was deposited on the p-metal pattern surface. After lift-off, we do lapping & polishing on the backside of the sample. RTA (rapid thermal annealing) begins by deposit the Ti/Pt/Au on the backside surface as the n-metal contact with the same process as we made the p-metal contact on the top side. After coating N-metal, then the sample put into RTA machine to do annealing process in certain conditions. In this process we have to do it carefully because if the temperature is too high, then it will break the backside of the sample. If this is happen, the laser performance will be very bad when the current is injected into the diode, even causing the diode could not lasing.

Then, after all the process was done, all samples were cut into many laser bars using the cutting machine and blue tape was used to prevent the metal lift-off of the metal-pad. The final SEM figure shows the uniformity of P-metal contact layer on the SiO₂ isolation layer covering the surface of the sample (Figure 7).

III. MEASUREMENT RESULTS

1) Light-Current Measurement Results

The light-current measurements have been conducted to know our laser

characteristics. This is actually a quite simple measurement. First, the current was injected from the Laser Diode controller to the laser device by probing the laser diode and then capturing the light output by integrating sphere which is connected directly to the optical power meter.

Table 1 records the best measurement results of light-current characteristics before the facets coating. Short analysis & discussion according to our knowledge about those results are given below.

Table 1. Light-Current Measurement Results (Laser characteristics)

Total Cavity Length (μm)	Taper Length (μm)	Threshold Current (mA)	Bias Current (mA)	Resistance (Ohm)	Output Power (mW)	Slope Efficiency (W/A)
200	0	16.5	53	16.53	2.628	0.07
	100	Failed	80	-	0,106	-
300	0	18.5	80	14.17	6.774	0.18
	100	Failed	80	-	0,074	-
	200	Failed	80	-	0.045	-
400	0	37.5	75	28.08	3.133	0.086
	100	Failed	80	-	0.085	-
	200	29	75	26.30	4.429	0.095
	300	39.5	75	22.84	2.422	0.065
500	0	19.5	90	22,71	6.485	0.09
	100	Failed	80	-	0.038	-
	200	22	80	16.80	8.566	0.16
	300	44.5	75	26.34	1.79	0.067
600	0	24.5	90	22.77	5.774	0.087
	200	25.5	90	23.29	2.646	0.073
	500	53.5	75	29.02	1.346	0.06
700	0	17	100	17.81	7.028	0,094
	200	32	120	20.80	6.623	0.078
	500	36	90	19.27	4.049	0.071
800	0	44	80	27.32	0.996	0.025
	500	33	80	25.19	5.197	0.108
900	0	Failed	80	-	0,148	-
	500	33	80	25.68	3.810	0.08

From the results above, we can see that no diode is lasing in the range of 200-500 μm total cavity length with 100 μm taper region. Really, this is quite strange because the whole measurement have shown us that the device tend to be lasing. So, how can we explain this problem? This problem maybe happens due to the bad metal contact on the top of the ridge waveguide or at the back side of the sample due to the higher temperature of RTA process. Those reasons will increase the leakage current because so much photon loss out of the resonant cavity laser. Since no device lasing in the length of 100 μm , the perfect comparison between 0, 100, 200, and 300 μm taper lengths in the same total cavity length couldn't be made. But, at least we agree that in the 400, 500, 600, and 700 μm total cavity length, the longer taper length will cause the higher threshold current. This conclusion is in harmony with many papers that mentioned everywhere.

The best measurement result of vertical-tapered is for the 500 μm total cavity length (including 200 μm taper's length), achieving 16% slope efficiency and 8.566 mW output power, respectively. And for the longer cavity length, it achieved the good result of about 5.2 mW output power and $\sim 11\%$ slope efficiency at the 800 μm total cavity length with 500 μm taper length. For non-taper laser, the best one is the 300 μm total cavity length with 18% slope efficiency and 6.774 mW output power, respectively. From those results, we can see that the way to produce the higher output power with the small threshold current is by keeping the constant cavity length of the laser is 300 μm and the different length between taper and total cavity length is also 300 μm .

Laser diodes with the same taper length of 500 μm producing the smaller threshold current at the total cavity length vary from 600 to 900 μm , but the output power is fluctuated. And for the range cavity length of 400 μm to 700 μm , the threshold current is going to increase linearly with the longer cavity length but the output power is also still fluctuated.

It was believed that it is possible to realize the higher output power of vertical-tapered waveguide FP-LD by diffusion-limited etching method as a low-cost and simple fabrication method. It means that this FP-LD can be a promised candidate light source for WDM-PON technology after the injection-locking method is used.

2) Injection-Locking Measurement Results

To get the single mode spectrum when applying to the injection-locking method, AR and HR-coating must be performed at both end facets of the laser diode. AR Coating at the front facet is about $\sim 5\%$ and HR Coating at the rear facet is about $> 90\%$.

Final measurement results are given here is about the injection-locking technique of the coating facets lasers. The first important measurement of this method is to get the highest coupling light from laser diode into the lens fiber. The output power of light coupling is measured by Power Meter (not shown in the diagram for simplicity) and its optical spectrum by OSA (Optical Spectrum Analyzer). The simple injection-locking measurement setup is given in Figure 8. First, we measure the lasing spectra

of the master laser and the multimode operation of the slave FP-LD. The master laser is a tunable laser source emitting at 1545.21 nm, which is close to the fourth side lasing-mode on the longer wavelength side mode of the slave laser.

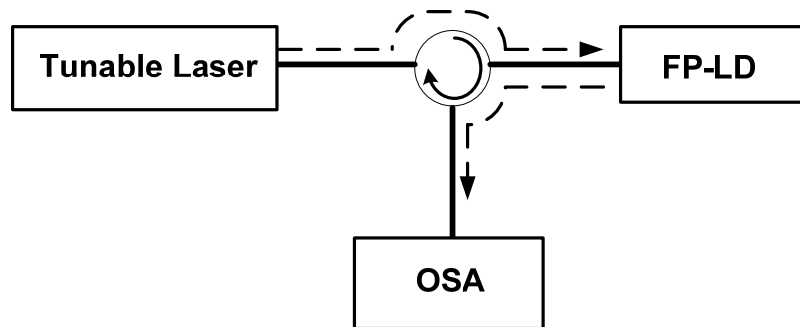


Figure 8. Simple Experimental Setup for Injection-Locking Measurements.

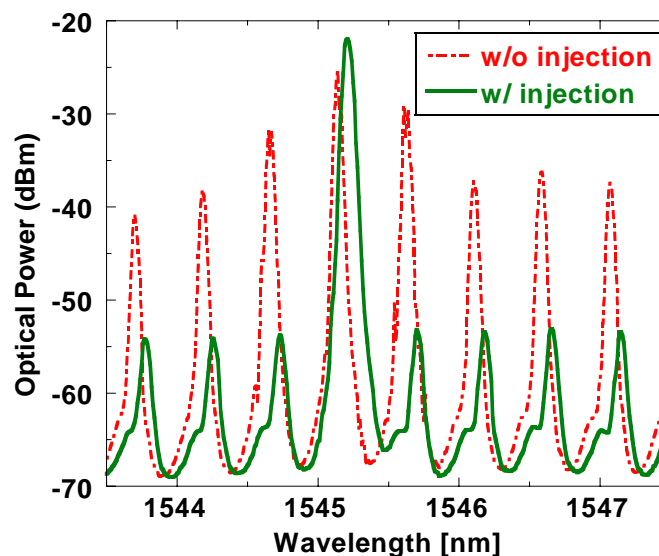


Figure 9. Measured optical spectra of the vertical-tapered FP-LD w/ and w/o injection-locking (500 μm cavity length with 200 μm taper).

In Figure 9, the dashed line (red color) shows the laser emission spectrum of the slave FP-LD with the main peak wavelength at 1545.14 nm. This is a typical FP laser spectrum and the side mode suppression ratio (SMSR) of this laser is about 4 dB.

Then, when the external laser master light is injected into the slave FP-LD which is biased above the threshold current, the injected light competes with the spontaneous emission of the laser for amplification. When the external light is strong enough and close to the eigen-frequency of the slave laser, it is amplified since there is a gain

available. At the same time it saturates the gain of the other modes and extinguishes all the other free-running modes. Once a perfect locking state is reached, all of the power of the slave laser is emitted at the optical frequency of the master laser as shown by the solid line (green color) in Figure 9.

Injection-locking greatly improves the SMSR of the slave FP-LD to be higher than 30 dB and shifts the wavelength from 1545.14 nm to 1545.21 nm. It means, this technique allows 0.07 nm wavelength detuning. This inter-mode injection locking can switch the information from the free-running mode to any side mode as long as the injection-locking condition is satisfied and can be used for optical wavelength conversion in the WDM channel selection.

CONCLUSION

Vertical InGaAsP/InP taper FP-LD was successfully realized using diffusion-limited etching method as a simple and low-cost fabrication technology. Under the optimal condition, we have the etching selectivity ratio of two between taper and non-taper region for test and real samples (good repetition results).

For the injection-locking applications, we proposed a wavelength-locked FP-LD by achieved a single-mode output from an uncooled and unisolated FP-LD by injecting a seed light from tunable laser diode. The side-mode suppression ratio (SMSR) increased from 4 dB to more than 30 dB and shifted the wavelength from 1545.14 nm to 1545.21 nm with tunable light source injection. This intermode injection-locking can switch the information from the free-running mode to any mode as long as the injection-locking condition is satisfied and can be used for optical wavelength conversion in the WDM channel selection. And we believed that this vertical InGaAsP/InP taper FP-LD could be a good and sufficient candidate as a low-cost ONU light source in WDM-PON transmission system and technology.

ACKNOWLEDGEMENTS

I am indebted so much for the advice and guidance of Dr. San-Liang Lee as my supervisor, for the valuable discussion about experimental method and fabrication of both Yen-Ting Pan and Yung-Jr Hung, for the labor of my good friend Yen-Ru Huang who provided all the SEM pictures, and for Dr. Shu-Chuan Lin who helped me so much to finish the injection-locking measurements.

REFERENCES

- [1] May, G. S. and Sze, S. M. (2004), *Fundamentals of Semiconductor Fabrication*, Chapter 1.2 & 1.3, John Wiley & Sons, Inc.
- [2] Cloutier, S. G. (ELEG340), "Semiconductor Devices," *Course Slides*.
- [3] Yariv, A. and Yeh, P. (2007) *PHOTONICS - Optical Electronics in Modern*

Communications, 6th ed, Oxford University Press.

- [4] Coldren, L. A. and Corzine, S. W. (1995), Diode Lasers and Photonic Integrated Circuits, Chapter 1.5, John Wiley & Sons, Inc.
- [5] Dutton, H. J. R. (1998), Understanding Optical Communications, *IBM International Technical Support Organizations*.
- [6] Moerman, I., Van Daele, P. P., and Demeester, P. M. (1997), A Review on Fabrication Technologies for the Monolithic Integration of Tapers with III-V Semiconductor Devices, *IEEE J. Select. Topics Quantum Electron.*, Vol (3), pp. 1308-1320.
- [7] Hadley, G. R. (1993), Design of Tapered Waveguides for Improved Output Coupling, *Photon. Technol. Lett.*, Vol (5), pp.1068-1070.
- [8] Ladele, E. O., Rahman, B. M. A., Wongcharoen, T, Obayya, S. S. A., and Grattan, K. T. V., (2001), Design optimization of monolithically integrated semiconductor spot-size converters for efficient laser-fiber coupling, *Proceedings EDMO*, Vienna, 2001.
- [9] Choudhury, A. N. M. M., Stanczyk, T.R., Richardson, D, and Oron, A. D. R. (2005), Method of Improving Light Coupling Efficiency Between Optical Fibers and Silicon Waveguides, *IEEE Photon. Technol. Lett.* , Vol (17), pp. 1881-1883.
- [10] Novera Optics, Inc, WDM-PON for the Access Network, *white paper*.
- [11] Xu, Z., Wen, Y. J., Zhong, W.-D., Chae, C.-J., Cheng, X.-F., Wang, Y., Lu, C., and Shankar, J. (2007), High-Speed WDM-PON using CW injection-locked Fabry-Perot laser diodes, *Optics Express*, Vol (15), pp. 2953-2962.
- [12] Belenky, G., Shterengas, L., Trussell, C.W., Reynolds Jr., C.L., Hybertsen, M.S., and Menna, R., Trends in semiconductor laser design: Balance between leakage, gain and loss in InGaAsP/InP MQW structures, January 2002 (Research Gate).
- [13] Kunii, T., Matsui, Y., Katoh, Y., and Kamijoh, T. (1995), Low Threshold Current and High Output Power Operation for 1.5 μ m GRINSCH Strained MQW Laser Diode, *Electron. Lett.*, Vol (31), pp. 282-284.
- [14] Hirayama, H., Miyake, Y., and Asada, M. (1992), Analysis of Current Injection Efficiency of Separate-Confinement-Heterostructure Quantum-Film Lasers, *IEEE J. Quantum Electron.*, Vol (28), pp. 68-74.
- [15] Moerman, I., D'Hondt, M., Vanderbauwhede, W., Coudenys, G., Haes, J., De Dobbelaere, P., Baets, R., Van Daele, P., and Demeester, P. (1994), Monolithic Integration of a Spot Size Transformer With a Planar Buried Heterostructure InGaAsP/InP-Laser Using the Shadow Masked Growth Technique, *IEEE Photon. Technol. Lett.*, Vol (6), pp. 888-890.
- [16] Simatupang, J. W., Wu, W. S., Lee, S. L. (2009), Relative Etching Rates of

Vertical Down Taper-Ridge Waveguide by Diffusion-Limited Etching, *Jurnal Sains dan Teknologi EMAS*, Vol (19), pp. 1-6.

- [17] Brenner, T. and Melchior, H. (1994), Local Etch-Rate Control of Masked InP/InGaAsP by Diffusion-Limited Etching, *J. Electrochem. Soc.*, Vol (141), pp.1954-1956.